# RAMAN SPECTROSCOPIC INVESTIGATIONS OF SWIFT HEAVY ION IRRADIATION EFFECTS IN SINGLE-WALLED CARBON NANOTUBES

A. Olejniczak[1,2)], V.A. Skuratov[1)], J.P. Lukaszewicz[2)]

[1)]*Joint Institute for Nuclear Research, Dubna, 141980, Russia*

[2)]*Faculty of Chemistry, Nicolaus Copernicus University, 87-100 Torun, Poland*

*e-mail: aolejnic@chem.uni.torun.pl*

In this study, we report the results on swift heavy ion irradiation effects in single-walled carbon nanotubes (SWNTs). Buckypapers, prepared of CVD grown, SWNTs were irradiated at room temperature with 167 MeV Xe ions to fluences in the range of $6 \cdot 10^{11}$ - $6.5 \cdot 10^{13}$ $cm^{-2}$ and investigated using Raman spectroscopy. We observed a rich set of features in the intermediate frequency mode region. Some of them, being defect-induced, resembled fairly well the phonon density of states (DOS) of nanocrystalline glassy carbon. Analysis of the RBM modes has shown that the broader metallic tubes are characterized by higher radiation stability than thinner semiconducting ones.

## Introduction

In recent years, the irradiation of carbon nanostructures with swift heavy ions (SHI) has been drawing an increasing attention. Swift heavy ions, due to their ability to depose huge amounts of energy in a small cylindrical volume surrounding an ion trajectory, offer the possibility for unique modification of composition, structural properties, and surface topology of the studied materials. The controlled introduction of low-dimensional defects seems to be one of the most important aspects of SHI interaction with nanostructured carbons, allowing for tuning their transport and optical properties.

The radiation damage in carbon-based materials is most commonly studied by Raman spectroscopy. Although the Raman spectra of CNTs are rich in a variety of dispersive and non-dispersive spectral features, the extent of radiation damage is typically quantified by the disorder parameter, expressed as the ratio of the D- and G-band intensities. Up till now, only little attention has been paid to the experimental investigation of the irradiation impact on the Raman features in the intermediate frequency region (IFM) [1]. This is mainly due to weak intensity of these features and the insufficient theoretical understanding of the underlying mechanisms [2,3,4]. The signals in the radial breaching mode (RBM) region, being characteristic of single-walled nanotubes (SWNTs), are rarely studied as well.

Our intention was to employ the spectral analysis of these Raman features (i.e., IFM and RBM modes) to get an insight into radiation-induced transformations in SWNTs. In particular, we focus on the differences in the radiation stability of metallic and semiconducting tubes.

## Experimental

Commercially available single-walled nanotubes, denoted as SWNTs (purity > 95 vol%, SWNT content > 90 vol%, diameter 1-2 nm, length 5-30 μm) were obtained from Nanostructured & Amorphous Materials. Nanotube thin films (so-called buckypapers) were prepared using the vacuum filtration method. Briefly, a portion of the nanotube powder was taken in an aqueous solution of Triton X-100 surfactant, sonicated in a low-power pulsed mode to form a stable suspension, and subsequently passed through a membrane filter. The resulting CNT films were then extensively washed with deionized water to remove any residual surfactant and dried.

Buckypapers were irradiated at room temperature with 167 MeV $^{132}Xe$ ions at the IC-100 FLNR JINR cyclotron. The incident electronic ($S_e$) and nuclear ($S_D$) stopping powers were calculated using the SRIM-2010 code, assuming the density of carbon nanotubes to be equal to that of graphite, and they were 17.3 and 0.08 keV/nm, respectively.

Raman spectra of virgin and irradiated specimens were recorded with a RamanMicro 300 spectrometer, using a 785 nm (1.58 eV) near-infrared laser source and a 50× objective lens. The spectral parameters were as follows: laser power 10 mW, resolution 2 $cm^{-1}$, CCD temperature –50 °C, and total integration time 600 s. To minimize detrimental effects due to possible sample and dose inhomogeneity, with each specimen, a point-by-point mapping was performed with 1 mm spacing on an area of 3 mm × 3 mm. The resulting subspectra were de-spiked, baseline corrected, and averaged.

## Results and discussion

Raman spectra in the intermediate frequency modes (IFM) region are shown in Fig. 1.

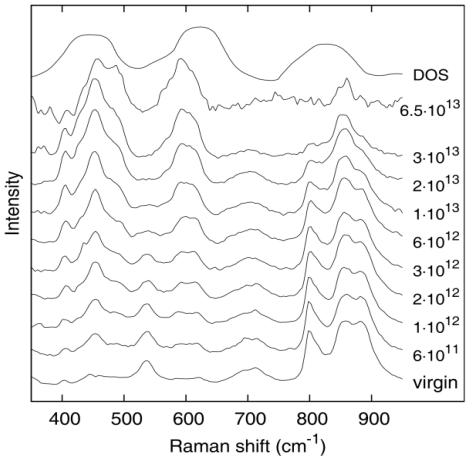


Fig. 1. IFM portions of the Raman spectra of virgin and Xe ion-irradiated SWNT specimens. Low frequency DOS of nanocrystalline glassy carbon, taken from ref. [5], is included for a comparison

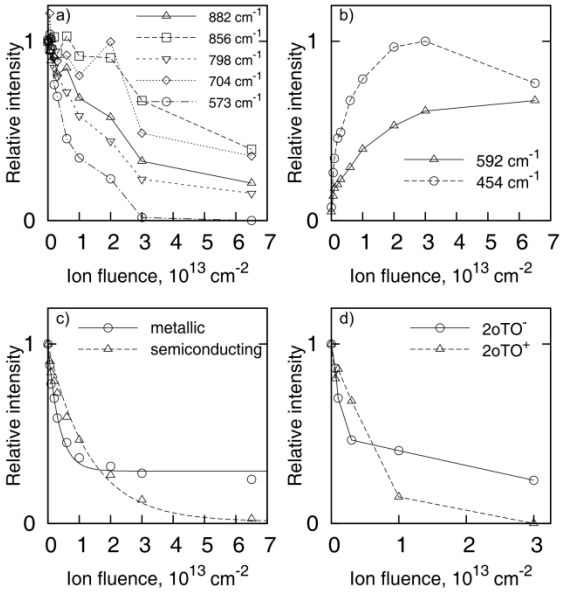


Fig. 2. Relative intensity change of IFM (a,b), RBM (c), and 2oTO (d) modes as a function of ion fluence

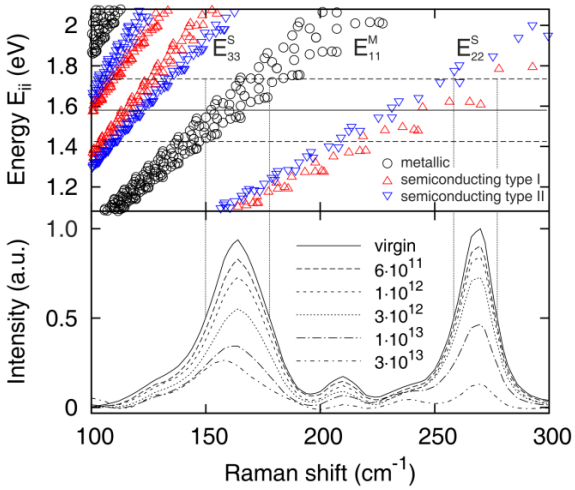


Fig. 3. The RBM spectra of virgin and irradiated SWNT specimens (a), Kataura plot showing optical energy $E_{ii}$ as a function of RBM frequency (b). The horizontal continuous line represents the laser excitation energy ($E_L$ = 1.58 eV), the dashed lines indicate the energy interval of 0.31 eV

The spectrum of unirradiated SWNTs exhibits a presence of several characteristic features. The two signals at 798 and 882 $cm^{-1}$, are ascribed to step-like dispersive modes, explained by a highly-selective second-order process involving a combination between an optic and an acoustic phonon [2]. Nondispersive first-order features are manifested as broad signals centered at 700 and 856 $cm^{-1}$. The first peak can be related to the out-of-plane transverse optical (oTO) and in-plane transverse acoustic (iTA) phonon branches near the M point of the graphite Brillouin zone. The second peak is assigned to the oTO phonon branch at the Γ point. The feature at 520 $cm^{-1}$ is most probably an overtone of the 266 $cm^{-1}$ RBM mode.

The relative intensity change of the IFM region signals as a function of the ion fluence is shown in Fig 2(a, b). As it can be seen, different types of the IFM signals behave differently with increasing ion dose. The intensities of the nondispersive features (700 and 856 $cm^{-1}$) do not undergo any significant changes upon irradiation up to a fluence of $2 \cdot 10^{13}$ ions/$cm^2$ (Figure 2(a)). This suggests that the bands are not influenced by defect concentration, and such a behavior has already been observed during nanotube functionalization [3]. At extremely high doses applied ($3 \cdot 10^{13}$-$6.5 \cdot 10^{13}$ ions/$cm^2$), significant decrease in the intensities of these peaks is observed, proving complete destruction of nanotube structure. In contrast, the step-like dispersive modes and RBM overtones decrease in their intensities over a whole ion fluence range and practically disappear at the highest fluence. Raman measurements of the irradiated specimens in the IFM region show the appearance of two new defect-induced peaks located at ~ 450 and ~ 600 $cm^{-1}$. Upon irradiation, the relative intensities of these peaks increase non-linearly with the irradiation dose and finally saturates (Fig. 2(b)). The assignments to these peaks made by different authors are reviewed in Ref. [4], however, their exact nature still remains unknown. In highly disordered carbon systems the Raman spectrum should reflect the phonon density of states (DOS). For a comparison we present in Figure 1, the low frequency DOS of nanocrystalline glassy carbon (*g*-C) determined experimentally from the inelastic neutron scattering data [5]. The DOS structure of *g*-C consists of three major bands with maxima at ca. 445, 620, and 825 $cm^{-1}$. The frequencies of the first two DOS bands and the respective defect-induced peaks are in fairly good agreement. The presence of the third feature in the Raman spectra could not be confirmed unequivocally, as the region is overlapped with both the step-like dispersive IFMs and oTO mode.

Now let us discuss the signals in the radial breaching mode (RBM) region. RBM modes are characteristic features of the first-order Raman spectrum of SWNTs. These features, usually appearing at the region of 100-300 $cm^{-1}$, result from the coherent motion of carbon atoms in the radial direction of the nanotube (i.e., contraction and expansion). As it can be seen in Fig. 3(a), the RBM portion of the spectrum of virgin SWNTs consists of two broad intensive peaks at ~160 and 266-270 $cm^{-1}$ and few other low intensive signals. It is well known that RBM features are due to the resonance Raman process, i.e. are observed only when the laser energy ($E_L$) is equal (or close to) the optical transition energy $E_{ii}$, characteristic for given structural indices (n, m). In Fig 3(b) we present the Kataura plot in which the optical transition energies $E_{ii}$ are plotted as a function of frequency. A comparison of the RBM spectral features with the Kataura plot shows that the 266-270 $cm^{-1}$ peak is due to semiconducting tubes (E22S transition), while the ~160 $cm^{-1}$ signal originate from metallic tubes (E11M transition). More detailed analysis allows one to assign the 266-270 $cm^{-1}$ peak to the 2n+m = 22 family with an average diameter of 0.9 nm, and its low-frequency shoulder with the intermediate 210 $cm^{-1}$ peak to the 2n+m = 25 family, characterized by the average diameter of 1.0 nm. Metallic tubes represented by the 160 $cm^{-1}$ signal are mainly broad ones, with average diameter

of ca. 1.5 nm. As it follows from Fig. 2(c), with increasing ion dose the intensities of all RBM modes undergo significant depletion. However, as the irradiation proceeds, significant difference in disappearance rate between the metallic and semiconducting tubes is visible. At low doses the destruction of metallic tubes proceeded at higher rate, but showed a tendency for saturation, and even at highest irradiation fluences their RBM signals were still visible. The irradiation of the semiconducting tubes, on the other hand, leads to complete disappearance of their RBMs. According to theoretical studies, the threshold energy for displacing a carbon atom, being chirality-dependent, decreases with the decrease in the nanotube diameter [6]. Thus, the defect formation rate is substantially higher for thin, highly curved SWNTs than for the broad ones. Another effect may come from the distinctively different properties of both types of nanotubes. Metallic nanotubes due to their better charge conductivity are capable to redistribute the deposited energy over the sample more rapidly. In this light, higher radiation stability of broader metallic tubes than thinner semiconducting ones seems to be natural consequence of the aforementioned properties. It should be pointed out here that the diameter-originating differences in the disappearance rates are visible also within nanotubes of a particular type. For semiconducting tubes it could be noticed that the signals of 2n+m = 25 family disappear slower than signals of 2n+m = 22 tubes, which results in a clear build-up of the peak at 240 $cm^{-1}$. Similarly, for metallic nanotubes irradiated at high doses, there is a build-up of low frequency peak at 140 $cm^{-1}$ and blue-shift of the main signal.

If our assumptions are valid, then the changes in the nanotube diameter distribution, resulting from more or less selective destruction process should also be reflected in the changes in frequency of the nondispersive IFM bands. According to theory, frequencies of both nondispersive IFM bands depend on the tube diameter, i.e. decrease with decreasing tube diameter. This dependence is not so clear in the case of 700 $cm^{-1}$ signal, as its frequency depends also on the tube chirality. In systems consisting of different tubes, this causes additional splitting and blurring, finally producing broad hump-shaped line. However, for present resonance conditions the ~ 850 $cm^{-1}$ oTO band should have a doublet-like structure with sub-peaks originating respectively from metallic ($E_{11}^{M}$ transition) and semiconducting ($E_{22}^{S}$ transition) tubes. As evidenced from Fig. 1, such a splitting is not observed, most probably due to unsatisfactory spectral resolution and overlapping with the step-like dispersive IFMs. Thus, we turn our attention to a low intensive feature near 1750 $cm^{-1}$, denoted here as 2oTO, which is an overtone of the oTO phonon. As the overtone frequency is approximately doubled, we expect that the inter-peak separation should be ca. doubled as well. A deconvolution procedure applied to the 2oTO band leads to a successful separation of two sub-peaks centered at 1756 ($2oTO^{-}$) and 1788 ($2oTO^{+}$) $cm^{-1}$ (Figure 4). The relative intensity changes of these

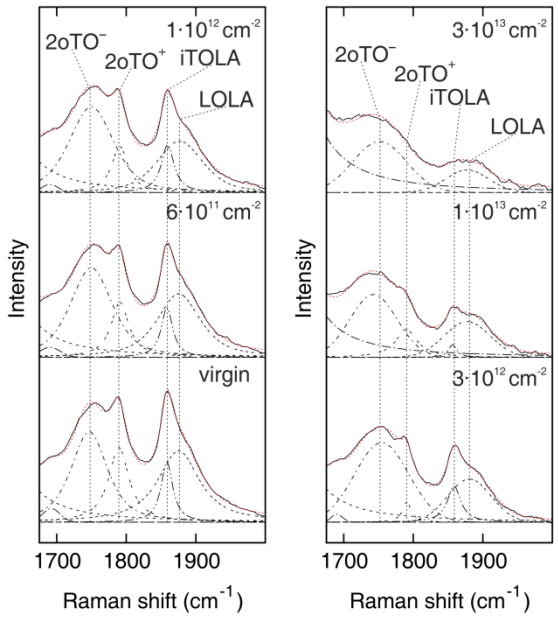


Fig. 4. Deconvolution of 2oTO Raman signal

peaks are plotted versus ion dose in Fig. 2(d). It could be seen that the $2oTO^{-}$ band, representing broader metallic tubes, is still present even for the highest irradiation dose, thus confirming our conclusions based on the analysis of the RBMs.

## Conclusions

We demonstrate that the analysis of weak, usually neglected, IFM modes enable to gain valuable information on radiation-induced phenomena in SWNTs. In particular, it was shown that SWNTs undergo significant damage upon irradiation with SHIs. The IFM portion of the Raman spectrum of highly disordered specimens resembled fairly well the phonon density of states (DOS) of nanocrystalline glassy carbon. Analysis of the RBM modes has shown that the broader metallic tubes are characterized by higher radiation stability than thinner semiconducting ones. However, the issue of the higher initial disintegration rate of metallic tubes remains unresolved within the curse of the present study and needs more excessive investigations.

## References

1. Skákalová *V., Maultzsch J., Osváth Z., Biró L.P., Roth S.* // Phys. Stat. Sol. – 2007. – 1. – No. 4. – P. 138.
2. *Fantini C., Jorio A., Souza M., Saito R., Samsonidze Ge.G., Dresselhaus M.S., Pimenta M. A.* // Phys. Rev. B. – 2005. – 72. – 8. – P. 085446.
3. *Fantini C., Pimenta M.A., Strano M.S.* // J. Phys. Chem. C. – 2008. – 112. – No. 34. – P. 13150.
4. *Roy D., Chhowalla M., Hellgren N., Clyne T.W., Amaratunga G.A.J.* // Phys. Rev. B. – 2004. – 70. – 3. – P. 035406.
5. *Li F., Lannin J.S.* // Appl. Phys. Lett. – 1992. – 61. – 17. – P. 2116.
6. *Krasheninnikov A.V., Banhart F., Li J.X., Foster A.S., Nieminen R.M.* // Phys. Rev. B. – 2005. – 72. – 12. – P. 125428.